BB

GSI

GSI-94-60
PREPRINT
SEPTEMBER 1994

RADIOCHEMICAL SEARCH FOR NEUTRON-RICH ISOTOPES OF NIELSBOHRIUM IN THE ^{16}O + ^{254}Es REACTION

M. SCHÄDEL, E. JÄGER, W. BRÜCHLE, K. SÜMMERER, E.K. HULET,
J.F. WILD, R.W. LOUGHEED, R.J. DOUGAN, K.J. MOODY

Gesellschaft für Schwerionenforschung mbH
Postfach 110552 · D-64220 Darmstadt · Germany

RADIOCHEMICAL SEARCH FOR NEUTRON-RICH ISOTOPES OF NIELSBOHRIUM IN THE $^{16}O + ^{254}Es$ REACTION

By M. Schädel, E. Jäger, W. Brüchle, K. Sümmerer

Gesellschaft für Schwerionenforschung mbH, D-64220 Darmstadt, FRG

E.K. Hulet, J.F. Wild, R.W. Lougheed, R.J. Dougan, and K.J. Moody

Lawrence Livermore National Laboratory,

Livermore, California 94551, USA

Element 107 / Nielsbohrium / Heavy ion reaction / ^{254g}Es target / Gas Chromatography / Transactinides /

Abstract

We have used on-line gas chromatography to search for new isotopes of element 107 near the deformed sub-shell at N = 162 and Z = 108. Enhanced nuclear stability is predicted for this region. ^{254g}Es was irradiated with ^{16}O at barrier energies to minimize the fusion hindrance in the entrance channel and to reduce the excitation energy of the compound nucleus to a minimum value. For half-lives between roughly two seconds and two minutes no signal for a positive identification of a new isotope of element 107 was detected. Consequently, only an upper cross-section limit of a few nanobarns was obtained. While this cross-section limit was too high to probe the influence of the predicted enhanced nuclear ground-state stability on the survival probability in the fission/evaporation competition, a very large cross-section enhancement would have been detectable.

1. Introduction

Over several years the concept of 'cold fusion' reactions [1] has proven to be very successful in synthesizing new elements with atomic numbers up to 109 [2]. Severe limitations, like an increasingly strong hindrance of the fusion process at the barrier [2-4] or the availability of target and projectile combinations, may restrict the further success of this approach. Overcoming the limitations of cold fusion reactions has become even more desirable in recent years. After the unexpected experimental observation of α-decay for the isotopes ^{265}Hs and ^{264}Hs [5,6], indicating a strong shell stabilization, various theoretical calculations have indicated a new region of deformed nuclei around neutron number N = 162 that are expected to be especially stable against spontaneous fission [7,8,9], with fission barriers as high as 5.5 to 7 MeV. Spontaneous fission half-lives are estimated to be hours and longer, and electron capture (EC)- and alpha-decay are predicted to be the dominant decay channels [8,10].

Fusion reactions with ^{254}Es as a target will lead to the most neutron-rich compound nuclei for elements above Z = 104, providing a means of investigating this region of enhanced nuclear stability. From extrapolation of measured transfer cross sections [11], one can assume that in this region, transfer cross-sections will begin to drop below the expected complete fusion-evaporation residue cross-sections. An additional advantage of using ^{254}Es targets is a reduction in fusion hindrance [12] because of the largest possible asymmetry in the entrance channel. In these reactions, with incident energies near the Coulomb barrier, the compound nucleus is formed with an excitation energy of about 40 MeV. One expects to find products from the 4n or 5n evaporation channels with highest cross sections; nevertheless, even these products are largely depleted by fission competition in the deexcitation process. Assuming no enhancement, we calculate cross sections of 90 pb and 50 pb [12] for ^{266}Ns and ^{265}Ns

in the reaction of ^{16}O on ^{254}Es. If the fission barriers in the N = 162 region are 5 to 7 MeV the overwhelming effect of prompt fission may be reduced and a larger fraction of evaporation residues might survive to reach the ground state.

We report an on-line gas-chromatographic experiment, based on the predicted high volatility of element 107, nielsbohrium (Ns), to search for ^{266}Ns produced from the ^{254}Es (^{16}O, 4n) reaction. The gas-chromatographic parameters were determined using rhenium, a homolog of nielsbohrium. The quality of the chromatographic separation and cross section limits for the production of ^{266}Ns are discussed.

2. Experimental

Ion beams of 113- and 116-MeV $^{16}O^{5+}$ from the 88-inch Cyclotron at the Lawrence Berkeley Laboratory passed through a 4.5 mg/cm^2 Mo window-foil, a volume of 0.7 mg/cm^2 nitrogen cooling gas, and the 4.49 mg/cm^2 Mo target substrate before entering a 50 μg/cm^2 ^{254g}Es target which contained about 8.8 μg/cm^2 of granddaughter ^{250}Cf. The beam energies entering the target material were 93 MeV and 96 MeV, respectively. The deposited electrical charge from the window outward to the beam dump was integrated and recorded periodically during the irradiations. The target was prepared by electrodepositing ^{254g}Es from an isopropanol solution of the chloride in a 3-mm diameter spot on the molybdenum substrate. This deposit was overplated with 20 μg/cm^2 of palladium to reduce transfer of the target material into the recoil chamber. Reaction products recoiling out of the target passed through the palladium overcoating as well as a 50 μg/cm^2 aluminum cover foil to further reduce the contamination by target material carried by the He jet.

After thermalization in 1.45 bar helium gas, recoil products attached themselves to KCl aerosol particles and were transported through a 1 mm diameter capillary approximately 6 m to the On-Line Gas Phase Separations Apparatus OLGA; see Ref. 13 for details of the set-up and the chemical procedures. Depending on various extreme assumptions about recoil range, recoil angle, and flow of the He through the 10 cm long cone installed for the confinement of the jet gas in a much larger chamber, a minimum transport time of about 1 s and a maximum transport time of 5 s were calculated. The He-gas flow was typically 0.75 l/min. Twenty percent oxygen was added to the He transport gas as a reactant to form oxide compounds with the reaction products either in the recoil chamber or, most likely, in the hot section (1050 ^{0}C) of the gas-chromatographic column. This section of the column was filled with a quartz wool plug to destroy all clusters and release the nuclear reaction products. A small water content equal to or less than 100 ppm was maintained in the gas to provide the best conditions for the formation of only one volatile species, as determined in test experiments with Re-tracers [13]. We assume that under these conditions nielsbohrium will form a volatile oxide compound [14,15], like the heavier group 7 elements. Similar conditions were utilized in a previous experiment to search for a new isotope of Ns [16]. This experiment was severely hampered by the use of a fission track detection method. From test experiments with Re tracer activities [13], we expected an overall yield of 56 %, which included the He(KCl) - cluster jet transport, the passage of Ns-oxides through the gas-chromatographic column and, after leaving the column, deposition on 0.67 mg/cm^2 Ni catcher foils coated with 50 μg/cm^2 Ta.

To reduce the small but continuously increasingly quantities of heavy actinides or other contaminants, which masked some parts of the α-spectra, we replaced the quartz tube approximately every four hours. To further reduce background radioactivities, we changed the reference position of the wheel after every hour of running time to collect

the activity on a different set of foils located on a wheel in OLGA. Four sets of 16 catcher foils each were mounted on the wheel, and were selected by the micro-processor which controlled the stepping of the wheel. The time required for the stepping motor to rotate and position the catcher wheel was 0.6 s. The positioning along the circumference of the wheel was equal to or better than ± 1 mm [13]. After a deposition interval of 5 s or 30 s, the collected activity was rotated between the first pair of surface barrier (SB) detectors. Seven pairs of 300-mm^2 SB-detectors were mounted along the perimeter of the wheel such that the angle between the collection position and the first detector pair and the angle between successive detectors was 45°. The detection efficiency was determined from a calibration source to be 24% for each detector on one side and 17% for the individual detectors on the opposite side of the catcher wheel. Signals from the preamplifiers were routed into the electronics of the MAD system [17]. Alpha energies were stored event-by-event together with the detector number and running time. These data were later converted into alpha spectra or sorted to search for α-α-correlations in time and/or detector and catcher foil number.

In one series of experiments with 93 MeV of ^{16}O ions (energy in the target) we accumulated doses of 9.33×10^{16} and 1.11×10^{16} particles with stepping times of 30 s and 5 s, respectively. In a second series of experiments with a projectile energy of 96 MeV doses of 2.54×10^{16} and 1.90×10^{16} particles were accumulated, again with stepping times of 30 s and 5 s, respectively. The ion energies were chosen to correspond to the calculated maxima of the excitation functions obtained with the evaporation code HIVAP for the production of ^{266}Ns, with parameters as described in Ref. 12, or with the SPIT code [18]. The corresponding Coulomb barrier (Bass) for the reaction is 94 MeV.

3. Results

The sum of all α-spectra from all detectors and experiments with a total dose of 1.49×10^{17} particles is shown in Fig.1. Below an energy of 7.5 MeV, where the intensity scale has been increased by a factor ten, the α-peaks can be assigned to well-known Fm and Md activities. The decay of the isotopes ^{252}Fm, ^{255}Fm, and ^{257}Md contribute to the broad peak centered at about 7.06 MeV, while the peak at 7.21 MeV is from the most intense α-line of ^{256}Md and some ^{254}Fm. The smaller peak on the high energy tail at 7.34 MeV comes from decays of ^{255}Md. All these isotopes are produced in transfer reactions from the ^{254}Es target with cross sections in the millibarn region [11], and a small portion pass through the gas-chromatographic column. The decontamination factor was better than 10^3, as determined by a comparison with directly measured α-activities from a separate experiment in which 1.91×10^{17} particles of 101 MeV ^{16}O were accumulated on a slightly thinner ^{254}Es target [11]. The presence of the heavy actinide products contributed a significant spontaneous fission background that made it impossible to search for SF decays of the Ns daughters. For comparison, the α-spectrum from this latter experiment is shown in Fig. 2. It also provides information on the ratio of the activities in the α-energy spectrum below and above 7.5 MeV from actinides produced in transfer reactions and, therefore, can be used as a guide in interpreting α-events between 7.5 and 8.95 MeV that were observed with poor statistics in the present experiment after the gas-chromatographical chemical separation (see Fig.1). Assignments to known isotopes can be made for all events below 8.95 MeV. However, in many cases, the assignments are not unique and some ambiguities remain. The α-events in the region between 7.46 MeV and 7.72 MeV are from low abundance α-lines of ^{256}Md, and up to 8.12 MeV from a series of ^{255}No α-lines. At 8.06 and 8.10 MeV ^{254}No and at 8.03 MeV ^{260}Lr may make a small contribution to the spectrum. Alphas up to 8.32 MeV are from ^{257}No. Above 10 MeV, directly produced 45-s

^{212m}Po is responsible for the peak at 11.67 MeV. The three events at 10.35, 10.47 and 10.62 MeV are from the ^{212}Bi beta-decay daughter activities of ^{212}Po. The two events at 11.15 and 11.78 MeV remain unassigned and they may be degraded fission products. Based on the decay properties theoretically predicted for $^{265\text{-}257}$Ns (see Table 1 and discussion in the next section) the most interesting energy region is between 8.4 and 9.2 MeV. Because of the importance of this region, and as some ambiguities that may remain in assigning the observed α-events to a known nuclides like ^{258}Lr, ^{262}Ha or ^{211,212}Po, we will discuss below each individual α-event observed in this region.

4. Discussion

We briefly summarize the expected decay modes of the isotopes $^{265\text{-}257}$Ns, listed in Table 1. The Q_α-values are derived from the most recent compilation of theoretical masses [19]. A comparison of theoretical masses from Ref. 19 with experimental masses of neighboring elements 104 and 106, where data are available for nearby isotopes, shows that the theoretical masses are, on the average, systematically too low by 0.65 MeV. For the Q_α-value we expect deviations of less than 0.5 MeV between experimental and theoretical data. Two semi-empirical formulas [20,21] have been used to calculate α-decay half-lives. Generally, results from both formulas are in reasonably good agreement with known α-decay half-lives [6]. The Q_{EC}-values are from Ref. 19, and the gross theory [22] has been used to calculate EC half-lives. No large differences are expected here from different mass formulas or microscopic theories. It is most difficult to predict spontaneous fission half-lives in this region of isotopes, especially for odd-A nuclei. From an empirical approach, looking at the rather long partial SF half-lives of the newly found neutron-rich nuclides ^{260}Md [23] and ^{261,262}Lr [24], or the observed α-decay of ^{264,265}108 [6], we expect that spontaneous

fission would not be a significant decay mode for the isotopes $^{265\text{-}267}$Ns. This expectation is corroborated by theoretical calculations [10,25].

To summarize, we expect that (i) α-decay will be the dominant decay mode for ^{265}Ns, with a maximum α-energy of 9.02 MeV and half-lives of up to about 10 s, (ii) for ^{266}Ns, α-decay will be the dominant decay mode with a maximum α-energy of 8.69 MeV and a half-life of up to about 20 s with a small probability for an EC-branch if the half-life for the α-decay is longer than 20 s, and (iii) for ^{267}Ns, EC decay may be as probable as α-decay with a maximum α-energy of 8.34 MeV and half-lives of up to about 4 min, the calculated EC half-life. The Q_α-values from semi-empirical systematics [26], which show a good agreement between experimental and calculated values for lighter isotopes, are about 0.8 MeV higher than the data from Ref. 19. We can take this as an indication for possibly higher α-energies and shorter half-lives than the ones in Table 1. The tabulated maximum α-energies were calculated for ground-state transitions from the Q_α-values of Ref. 19. In our experiment we expect to observe the main α-groups at lower energies, from favoured decays to states with excitation energies of hundreds of keV.

We return to the discussion of the observed α-events in the energy region between 8.4 and 9.2 MeV (see Fig.3 and Table 2). No correlated, successive α-decays were observed between any two alpha events in this region. Possible candidates for the assignment of three alphas in the region between 8.52 and 8.62 MeV are ^{262}Ha and ^{258}Lr [27] produced either in an (^{16}O, α4n) or transfer reactions, or as the decay product from a ^{266}Ns α-decay. Only the events at 8.52 MeV and, with a much lower probability, the one at 8.54 MeV may originate from the decay of directly produced ^{258}Lr because of the short half-life and the time difference (Δt) between end of collecting the activity (EOC) and the observed decay (decay) as listed in Table 2. An assignment of both the

8.52 MeV and 9.08 MeV events to ^{212m}Po can be ruled out because of the 2% relative intensity of the 8.52 MeV and 1% of the 9.08 MeV lines are known compared to 97% at 11.6 MeV. A maximum of only two events in this region (11.67 and 11.78 MeV in Fig.1), were observed in different runs and these could be attributed to ^{212m}Po.

The events between 8.68 and 8.82 MeV probably belong to ^{212}Po coming from the parent ^{212}Bi. The isotopes ^{259}104 and ^{257}Lr can be excluded because their half-lives are too short and no precursors with sufficiently long half-lives are known.

The group at 8.90 MeV originates from ^{211m}Po. An assignment to ^{261}Ha can be excluded as long as there is no indication for the existence of a longer-lived precursor ($T_{1/2} \geq 20$ s).

There is no indication that any α-event below 8.92 MeV originates from the decay of an element 107 isotope, and assignments to known isotopes, even if not totally conclusive in all cases, are possible. More interesting are the four events above 8.95 MeV. A remaining candidate for the two events at 8.98 and 9.03 MeV may be ^{257}104. This does not seem to be very likely because only production mechanisms with very low cross sections like multinucleon transfer from ^{254}Es or a ^{250}Cf (^{16}O, 5n) ^{261}106 reaction followed by α-decay to ^{257}104 can lead to this isotope. An additional depletion of element 104 products is expected in the chemical separation. Therefore, we have no assignments for the four α-events at about 9.04 MeV. Because we observed no correlated, successive α-decays into the region of known nuclei (mother-daughter correlation), we are not able to assign any event to the decay of an isotope of element 107. We have taken the energy window from 8.95 to 9.08 MeV for upper-limit cross-section calculations. The result, as a function of an assumed half-life, is shown in Fig. 4. For half-lives below 20 s, the lowest limits result from the experiments with

5 s stepping time. No events were observed in these runs but 3 events have been assumed in order to calculate cross section limits with a 95% confidence level. The dashed line in Fig. 4 represents the result with the assumption of a 5 s transport time for the reaction products from the target to the OLGA, while the solid line characterizes a 1-s transport time. These times have been taken as the two extreme limits, whereas the actual transport time should lie somewhere in between. The kink in the solid line at 20-s half-life and the shallow dip towards longer half-lives results if one calculates upper-limit cross sections with the four α-events observed during the runs with a 30-s stepping time. In this case, nine events were used in calculating a 95% confidence level. For the longer half-lives, one obtains only a factor of 1.33 difference in the calculated limits whether the runs with 5 s stepping time and zero observed events or the ones with 30 s stepping time and four observed events are taken.

4. Conclusions

We have observed no correlated, successive α-decays of an unknown isotope into the region of known nuclei, thus we are not able to assign any events to an isotope of element 107. Upper-limit cross sections of a few nanobarns have been calculated for isotopes with an assumed half-life of about two seconds or longer. These upper limits are larger than the calculated ones by more than an order of magnitude.

Presently, an unequivocal interpretation of this result is not possible. Although it is unlikely, we can not exclude the possibility that the $^{265\text{-}267}$Ns half-lives are shorter than two seconds. We have found no large enhancement in the probability for reaction products to reach the ground state in this region of a predicted increased nuclear stability. If there is no enhancement of production cross sections from a stabilization of the deformed nuclei around N = 162, then one would expect a cross section for the

production of ^{266}Ns in a 4n-reaction of about 250 pb from an extrapolation of experimental data and about 100 pb from calculations with the evaporation code HIVAP [12]. From these calculations one would also expect a factor of ten increase in cross section with each MeV increase of shell stability.

It has been shown that gas-chromatographic separation techniques, with separation factors from actinides of 10^3 and higher, are applicable to searches for new isotopes of the heaviest elements with half-lives of a few seconds or longer.

For isotopes with half-lives of a few seconds or longer, cross section limits of 100 pb are still accessible to radiochemical experiments. The integrated beam intensities can be increased by more than one order of magnitude, technical improvements like shorter rotation times together with much shorter dead times of the rotating wheel and a higher detection efficiency are feasible, and the decontamination factor of the chemical separation can be improved by at least one order of magnitude. Half-lives below one second may require the use of physical techniques like recoil separators.

Acknowledgements

We would like to thank the staff and crew of the 88-inch cyclotron in Berkeley for their assistance in setting up the experiment and providing the oxygen beams. It is a pleasure for four of us (MS, WB, EJ, KS) to acknowledge the hospitality of the LLNL Heavy Element Group and that of LBL. We are indebted for the use of the target material to the Office of Basic Energy Sciences, U.S. Department of Energy, through the transplutonium production facilities of the Oak Ridge National Laboratory.

This research was performed under the auspices of the U.S. Department of Energy by the Lawrence Livermore National Laboratory under contract No. W-7405-Eng-48.

Figure Captions

Fig.1. Spectrum of all α-events between 7.0 MeV and 12.0 MeV observed in all runs at 93 MeV and 96 MeV projectile energy and with 5 s and 30 s stepping times. The part below 7.5 MeV is reduced by a factor of ten.

Fig.2. Alpha spectrum obtained without chemical separation from an experiment with 101 MeV ^{16}O as described in Ref. 9.

Fig.3. Spectrum of all α-events between 8.4 and 9.2 MeV as in Fig. 1.

Fig.4. Upper limit cross sections (95% conf. level) for the production of the isotopes $^{265\text{-}267}107$ as a function of an assumed half-life in reactions of ^{254}Es as a target with ^{16}O ions at the barrier. The dashed curve represents the limit for a 5 s and the solid curve for a 1 s transport time from the target to the OLGA.

References

1. Oganessian, Yu.Ts., Iljinov, A.S., Demin, A.G., Tretyakova, S.P.,
   Nucl. Phys. **A239**, 353 (1975)
2. Armbruster, P.,
   Ann. Rev. Nucl. Part. Sci. **35**, 135 (1985)
3. Blocki, J.P., Feldmeier, H., Swiatecki, W.J.,
   Nucl. Phys. **A459**, 145 (1986)
4. Iljinov, A.S., Oganessian, Yu.Ts., Cherepanov, E.A., Demin, A.G.,
   Nuovo Cimento **101(A)**, 225 (1988)
5. Armbruster, P., 1984, "Discovery of Element 108. The Island of α-Active Nuclei Beyond Element 105" In: From Nuclei to Stars, Proc. XCI Corso, Soc. Italiana di Fisica, Bologna, (North-Holland , Amsterdam) pp.221-240 (1985)
6. Münzenberg, G., Armbruster, P., Berthes, G., Folger, H., Heßberger, F.P., Hofmann, S., Keller. J., Poppensieker, K., Quint, A.B., Reisdorf, W., Schmidt, K.-H. Schött, H.-J., Sümmerer, K., Zychor, I., Leino, M.E., Hingmann, R., Gollerthan, U., Hanelt, E.,
   Z. Phys. A - Atomic Nuclei **328**, 49 (1987)
7. Möller, P., Leander, G.A., Nix, J.R.,
   Z. Phys. A - Atomic Nuclei **323**, 41 (1986)
8. Böning, K., Patyk, Z., Sobiczewski, A., Cwiok, S.,
   Z. Phys. A - Atomic Nuclei **325**, 479 (1986)
9. Patyk, Z., Sobiczewski, A.
   Nucl. Phys. **A533**, 132 (1991)
10. Patyk, Z., Skalski, J., Sobiczewski, A., Cwiok, S.,
    Nucl. Phys. **A502**, 591c (1989)

11. Schädel, M., Brüchle, W., Brügger, M., Gäggeler, H., Moody, K.J., Schardt, D., Sümmerer, K., Hulet, E.K., Dougan, A.D., Dougan, R.J., Landrum, J.H., Lougheed, R.W., Wild, J.F., O'Kelley, G.D.,
Phys. Rev. **C33**, 1547 (1986)

12. Reisdorf, W., and Schädel, M.,
Z. Phys. A - Hadrons and Nuclei **343**, 47 (1992)

13. Schädel, M., Jäger, E., Schimpf, E., Brüchle, W., Sümmerer, K.,
submitted for publication to Radiochim. Acta, 1994

14. Keller, O.L. Jr., Seaborg, G.T.,
Ann. Rev. Nucl. Sci. **27**, 139 (1977)

15. Silva, R.J., 1986,
In: The Chemistry of the Actinide Elements,
eds. Katz, J.J., Seaborg, G.T., Morss, L.R.,
2nd ed., Vol. 2, Chapman and Hall, London, pp. 1085-1117

16. Zvara, I., Domanov, V.P., Hübener, S., Shalaevskii, M.R., Timokhin, S.N., Zhuikov, B.L., Eichler, B., Buklanov, G.V.,
Sov. Radiochem. **26**, 72 (1984)

17. Dougan, R.J., Lougheed, R.W., Hulet, E.K., Bethune, G.R.,
LLNL Nuclear Chemistry Division FY84 Annual Report, UCAR 10062-84/1, p. 2-15 (1984)

18. Haynes, G.R., Leyba, J.D., Hoffman, D.C., private communication

19. Möller, P., Nix, J.R., Myers, W.D., and Swiatecki, W.J.,
"Nuclear Ground-State Masses and Deformations", accepted for publication in At. Data Nucl. Data Tables (1994)

20. Poenaru, D.N., Ivascu, M.,
J. Physique **44**, 791 (1983)

21. Viola, V.E., Seaborg, G.T.,

Inorg. Chem. **28**, 741 (1966)

22. Takahashi, K., Yamada, M., Kondoh, T.,

At. Data Nucl. Data Tables **12**, 101 (1973)

23. Lougheed, R.W., Hulet, E.K., Dougan, R.J., Wild, J.F., Dupzyk, R.J., Henderson, C.M., Moody, K.J., Hahn, R.L., Sümmerer, K., Bethune, G.,

J. Less-Common Met.**122**, 461 (1986)

24. Hulet, E.K.,

Proc. Int. School-Seminar on Heavy Ion Physics, Dubna, 1989, and preprint UCRL-100763 (1989)

25. Smolanczuk, R., Skalski, J., Sobiczewski, A.,

GSI Scientific Report 1993, GSI-94-1 (1994) p. 80

26. Kolesnikov, N.N., Demin, A.G.,

Report VINITI Dep. No. 7309-1387, Tomsk, 1987, unpublished

27. Schädel, M., Brüchle, W., Schimpf, E., Zimmermann, H.P., Gober, M.K., Kratz, J.V., Trautmann, N., Gäggeler, H., Jost, D., Kovacs, J., Scherer, U.W., Weber, A., Greorich, K.E., Türler, A.,Czerwinski, K.R., Hannink, N.J., Kadkhodayan, B., Lee, D.M., Nurmia, M.J., and Hoffman, D.C.

Radiochim. Acta **57**, 85 (1992)

Table 1: Theoretically Expected Decay Mode Characteristics of $^{265-267}$Ns

^{265}Ns			^{266}Ns			^{267}Ns			Re1	
Q_α [MeV]	E_α [MeV]	$T_{1/2}(\alpha)$ [s]	Q_α [MeV]	E_α [MeV]	$T_{1/2}(\alpha)$ [s]	Q_α [MeV]	E_α [MeV]	$T_{1/2}(\alpha)$ [s]	Q_α	$T_{1/2}$
9.16	9.02	0.4 6.3	8.82	8.69	19.1 14.2	8.47	8.34	100 1370	19	20 21
Q_{EC} [MeV]		$T_{1/2}$ (EC) [s]	Q_{EC} [MeV]		$T_{1/2}$ (EC) [s]	Q_{EC} [MeV]		$T_{1/2}$ (EC) [s]	Q_{EC}	$T_{1/2}$
3.65		78	4.66		97	2.95		197	19	22

Table 2: List of α-events between 8.4 and 9.2 MeV

E_α (MeV)	E (^{16}O) (MeV)	Δt (EOB-decay) (s)	E_α (MeV)	E (^{16}O) (MeV)	Δt (EOB-decay) (s)
8.52	93	10.8	8.81	93	23.5
8.54	93	17.2	8.82	96	116.2
8.62	93	93.6	8.90	93	131.6
8.68	96	122.1	8.91	93	107.1
8.69	93	93.7	8.91	93	44.5
8.72	93	161.1	8.91	93	7.5
8.72	93	100.0	8.92	96	36.9
8.74	93	19.6	8.98	93	28.3
8.74	93	193.6	9.03	93	42.1
8.80	96	4.0	9.04	96	180.0
			9.08	93	19.8

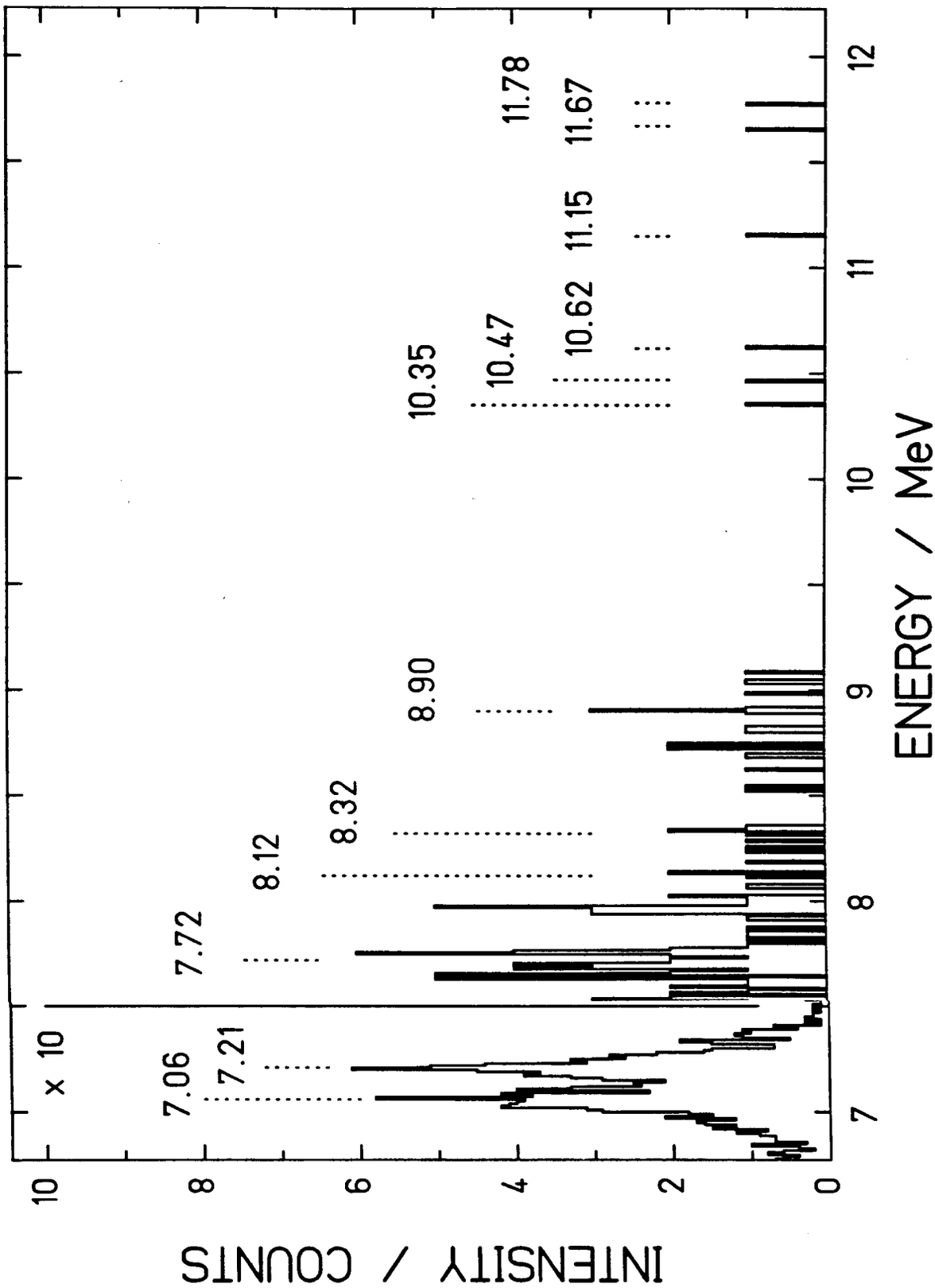
INTENSITY / COUNTS
ENERGY / MeV
x 10
7.06
7.21
7.72
8.12
8.32
8.90
10.35
10.47
10.62
11.15
11.67
11.78

Fig.1

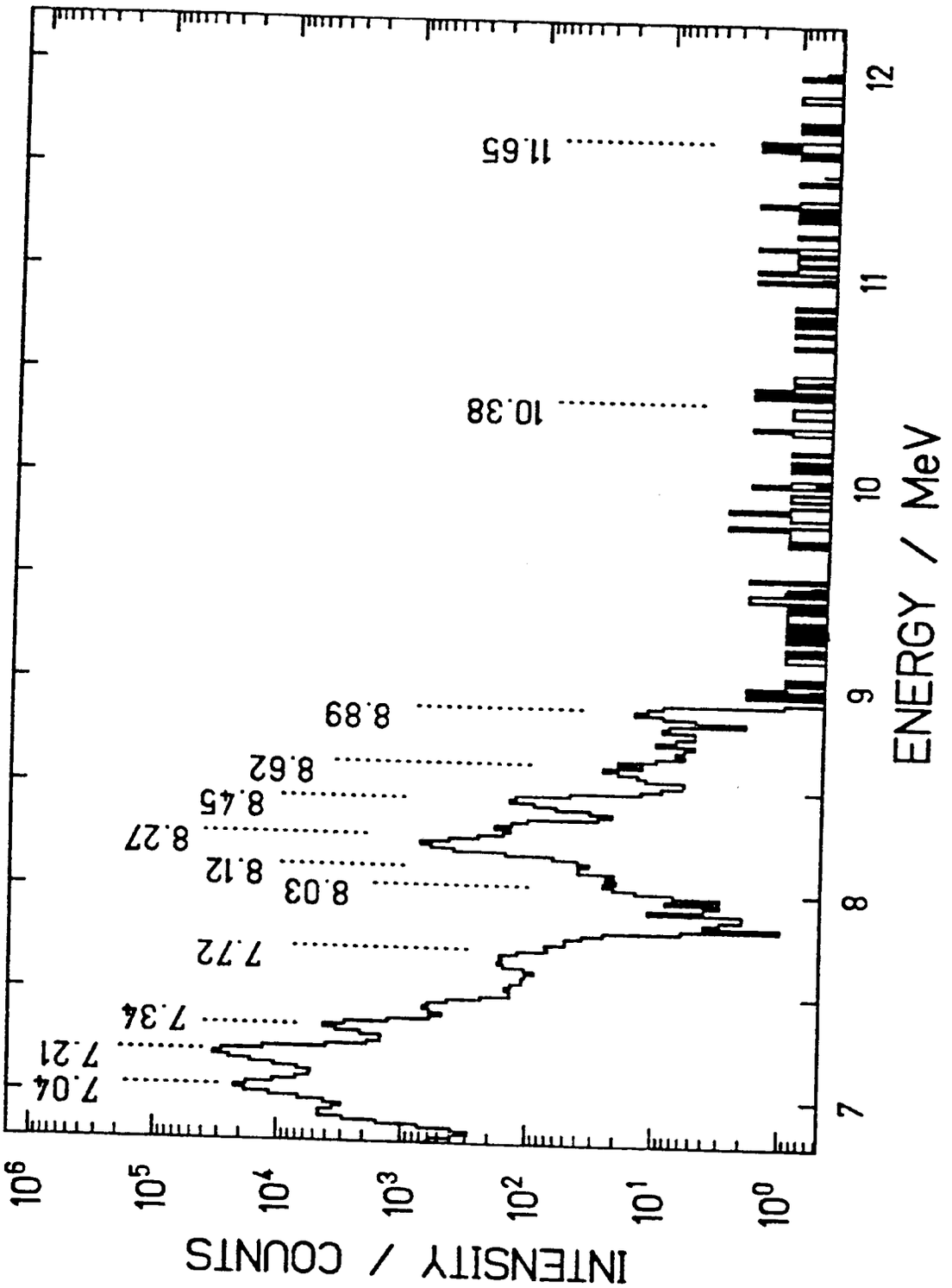
INTENSITY / COUNTS
10^6
10^5
10^4
10^3
10^2
10^1
10^0
7
8
9
10
11
12
ENERGY / MeV
7.04
7.21
7.34
7.72
8.03
8.12
8.27
8.45
8.62
8.89
10.38
11.65

Fig 2

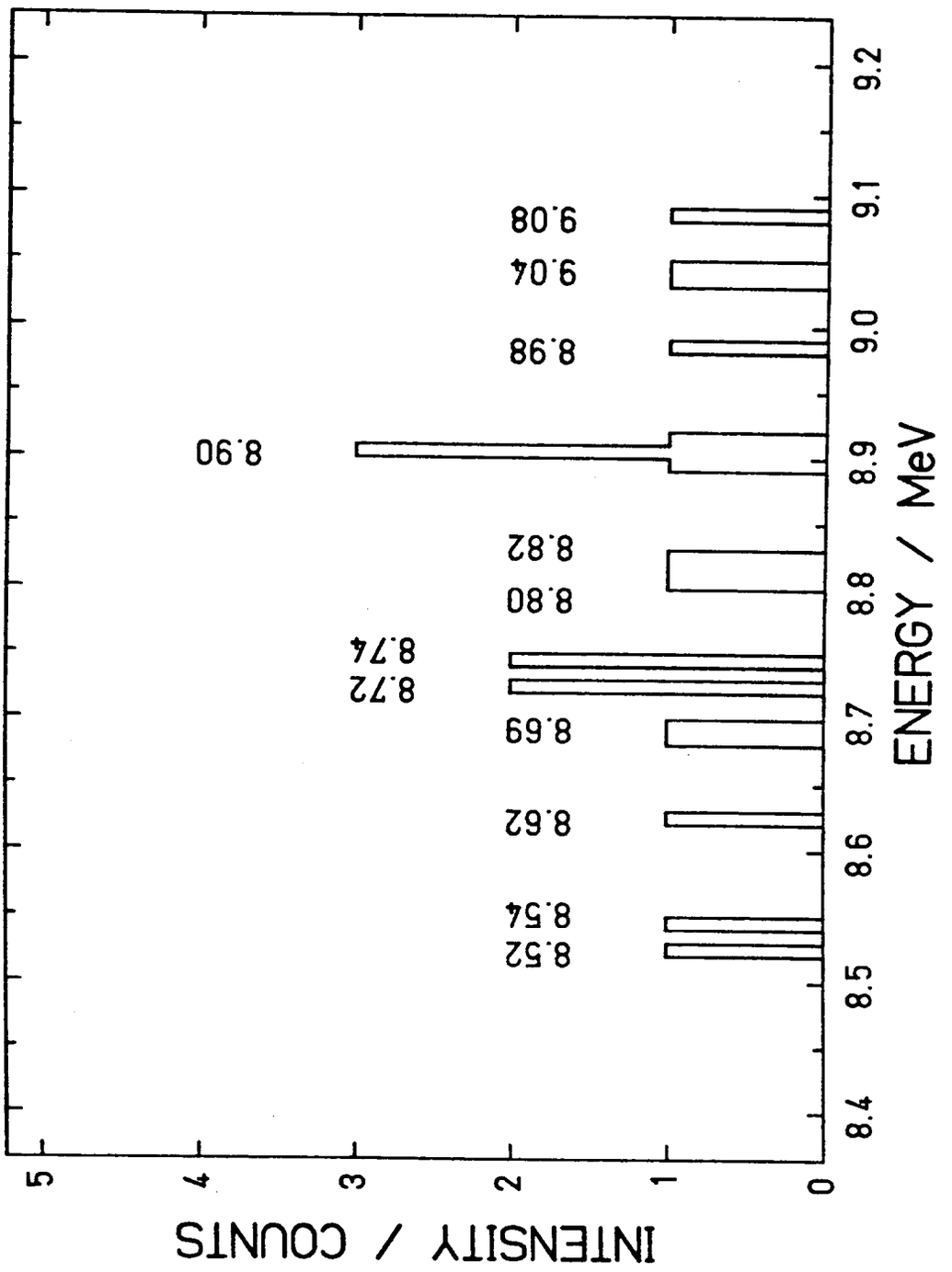
INTENSITY / COUNTS
0
1
2
3
4
5
ENERGY / MeV
8.4
8.5
8.6
8.7
8.8
8.9
9.0
9.1
9.2
8.52
8.54
8.62
8.69
8.72
8.74
8.80
8.82
8.90
8.98
9.04
9.08

Fig. 3

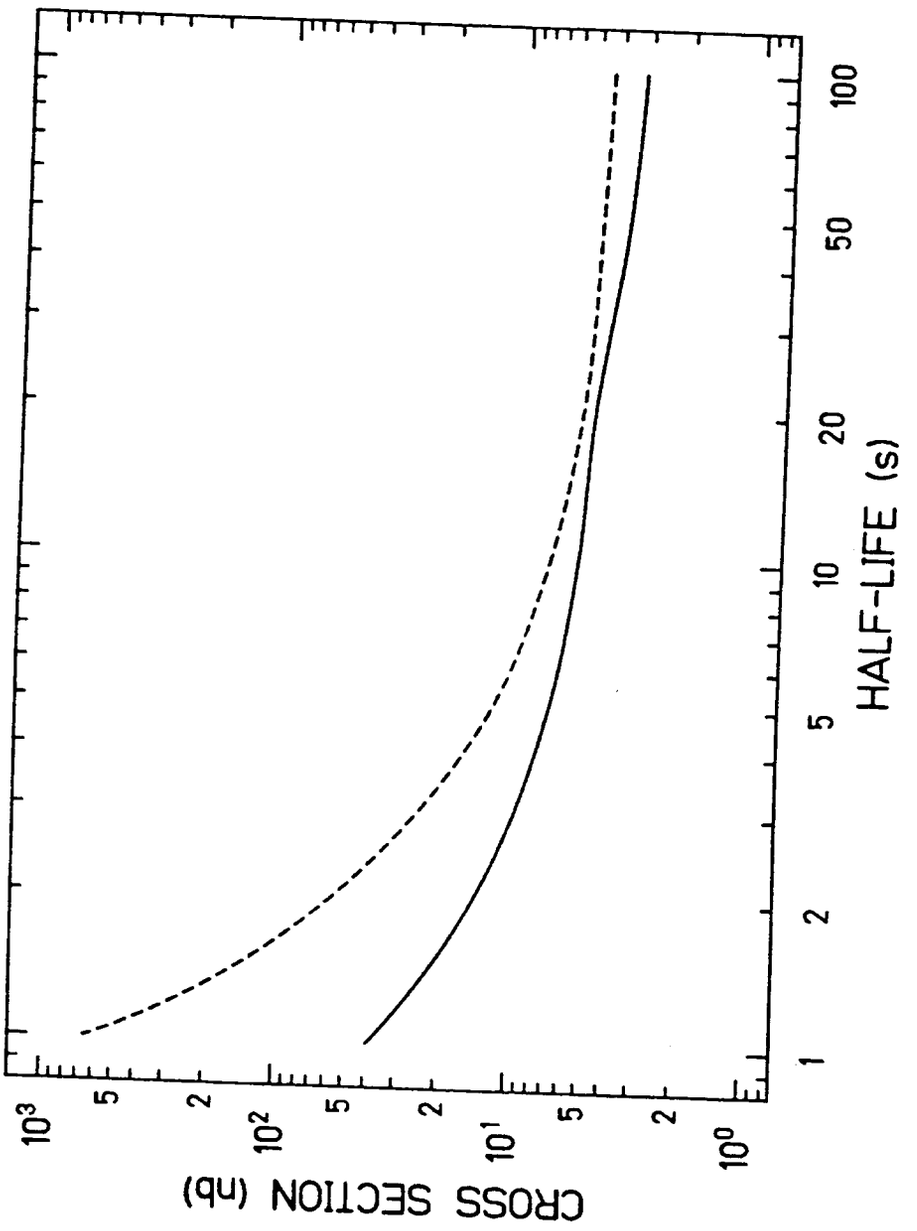
CROSS SECTION (nb)
10^3
5
2
10^2
5
2
10^1
5
2
10^0
HALF-LIFE (s)
1
2
5
10
20
50
100

Fig. 4